

Use of Simulation To Optimize NO_x Abatement by Absorption and Selective Catalytic Reduction

Andrew J. Sweeney and Y. A. Liu*

Honeywell Center of Excellence in Computer-Aided Design, Department of Chemical Engineering, Virginia Polytechnic Institute and State University, Blacksburg, Virginia 24061

This paper describes the development of an ASPEN PLUS simulation model for a commercial NO_x abatement system involving both absorption and selective catalytic reduction (SCR). The model helps identify operator guidelines and retrofit options needed to enable the commercial system to operate efficiently during surges in NO_x-laden fumes without incurring costly fines. The resulting model applies a reactive-distillation module with a practical reaction set for NO_x absorption and implements a kinetic model for SCR. The simulation results agree well with both design specifications and literature data and provide practical insights for optimum operation and economical retrofits of the commercial system.

1. Introduction

The system under analysis involves two key processes: absorption and selective catalytic reduction (SCR). The absorption of nitrogen oxide (NO_x) gases, particularly NO₂, into aqueous solutions is important in both nitric acid production and the abatement of NO_x-laden effluent streams for environmental protection.¹ Downstream, SCR removes NO_x by injecting ammonia into the flue gas, where chemical reactions in the presence of a catalyst convert NO to nitrogen and water.²

Previous studies have investigated NO_x absorption and SCR individually using accurate but highly complex mass-transfer and reaction-kinetics calculations. They have not, however, thoroughly treated these two processes in combination and, consequently, little literature exists on the subtleties of linking these two distinct, emerging technologies. Yet, more and more chemical and environmental engineers in the field have begun exploiting opportunities to effectively couple the processes to maximize NO_x removal, making the need for more research critical.

Such a system is, in fact, already in place at the Radford Facility and Army Ammunition Plant (RFAAP), Radford, VA. In response to the knowledge gap in the literature, this work simulates the multimillion-dollar RFAAP NO_x abatement system to develop operator guidelines and low-cost retrofit options that will ensure efficient operation during surges in NO_x-laden fumes that currently produce higher-than-allowed NO_x outflows. This effort will avoid frequent shutdowns and costly fines of up to \$25 000/day from the Virginia Department of Environmental Quality (VDEQ) for NO_x outflows above the hourly average limit of 125 ppm by volume (ppmv).

Combining real plant data with literature parameters, we have developed an ASPEN PLUS model that simulates system performance, and the results compare favorably with both plant data and literature for processes with similar conditions. The simulation predicts system sensitivity to various process variables and

suggests retrofit options for RFAAP that can increase the operating efficiency. Importantly, its success makes it an effective starting point for modeling similar situations.

2. NO_x Abatement Process at RFAAP

The RFAAP process receives NO_x-rich fumes from the nitrocellulose production line on site. The abatement system combines an absorber tower to remove NO₂ and an SCR catalyst vessel to remove NO.

Specifically, the absorber removes most of NO₂ in the NO_x fumes and converts a portion to nitric acid. The remaining NO_x fumes proceed to a catalyst vessel, where ammonia reduces NO_x to atmospheric nitrogen, N₂. From the catalyst vessel, the gases go to the stack and out to the atmosphere. Figure 1 shows the process, with stream values drawn from the design specifications.

The absorber houses 16 bubble-cap trays in the upper portion of the tower and 2 spray-scrubber sections in the bottom. The NO_x-laden fumes enter the bottom of the tower and contact with a mist of weak nitric acid. Filtered water enters at the top and flows down as the fumes flow up. The fumes leave the top of the column and enter a demister tank, where they impinge on stainless steel mesh screens, removing the entrained liquid that could damage the catalyst vessel.

The SCR reaction occurs at 316 °C. The fumes leave the absorber at 27 °C and are heated in three stages: (1) a steam preheater heats the vapor stream to 38 °C; (2) a heat exchanger, called an economizer, uses post-reaction gases to heat the stream to approximately 177 °C; and (3) a direct-fired heater uses natural gas combustion to increase the temperature to 316 °C.

3. ASPEN PLUS

ASPEN PLUS is currently the most popular chemical process simulation software used. Given its wide use, we choose it for this process to determine if it could simulate the complexities of NO_x absorption and SCR. Several factors present a challenge when considering the viability of the simulation software in this process. For example, what are the chemical reactions important to NO_x absorption and how are those reactions imple-

* To whom correspondence should be addressed. Phone: (540) 231-7800. Fax: (540) 231-5022. E-mail: Design@Vt.Edu.

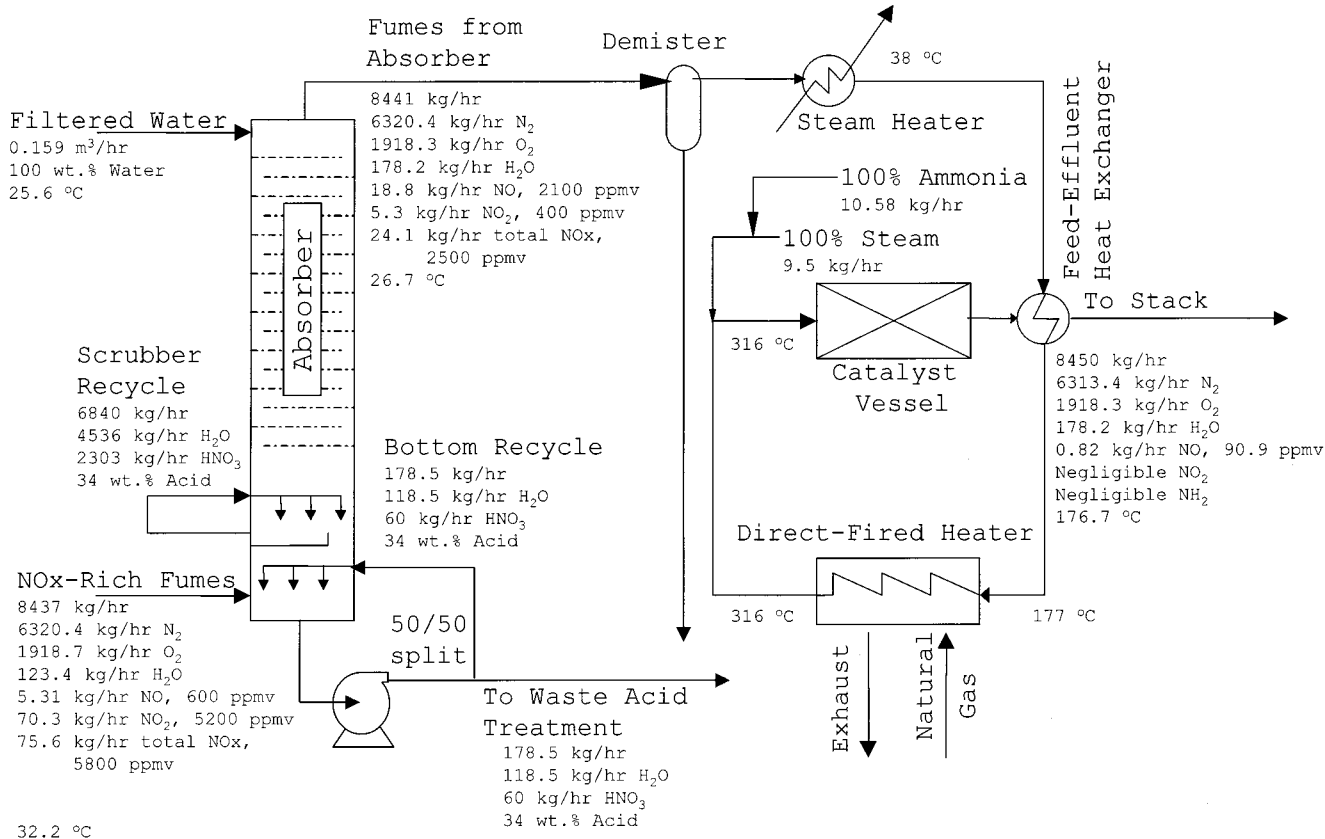


Figure 1. Block flow diagram of the NO_x abatement system provided by RFAAP.

Table 1. Full Reaction and Absorption Mechanism for NO_x and Water^{3,a}

N ₂ O ₄ pathway		N ₂ O ₃ pathway		NO ₂ pathway	
2NO + O ₂ ↔ 2NO ₂	(1)	NO + NO ₂ ↔ N ₂ O ₃	(6)	3NO ₂ + H ₂ O ↔ 2HNO ₃ + NO	(10)
2NO ₂ ↔ N ₂ O ₄	(2)				
N ₂ O ₄ (g) ↔ N ₂ O ₄ (l)	(3)	N ₂ O ₃ (g) ↔ N ₂ O ₃ (l)	(7)	NO ₂ (g) ↔ NO ₂ (l)	(11)
				HNO ₃ (g) ↔ HNO ₃ (l)	(12)
N ₂ O ₄ + H ₂ O ↔ HNO ₃ + HNO ₂	(4)	N ₂ O ₃ + H ₂ O ↔ 2HNO ₂	(8)	2NO ₂ + H ₂ O ↔ HNO ₃ + HNO ₂	(13)
3HNO ₂ ↔ HNO ₃ + H ₂ O + 2NO(g)	(5)	2HNO ₂ + O ₂ ↔ 2HNO ₃	(9)		

^a (l) refers to a liquid-phase component, and (g) refers to a gas-phase component.

mented in the software? How do we deal with the electrolyte species in the liquid phase inside the absorption column? How do we handle combined reactions and separation in an absorption column? We shall address these and other fundamental and practical issues below.

4. Simulating NO_x Absorption: Practical Reaction Set

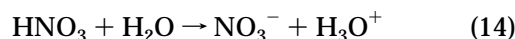
The conditions for treating effluents from combustion sources generally preclude using absorption but are ideal for SCR. However, SCR does not deal with NO₂ as efficiently as NO. Therefore, cases such as RFAAP require both processes. Importantly, unlike most gas absorption, NO_x absorption is driven primarily by chemical reaction, while the rate-limiting step is interfacial mass transfer. Table 1 lists the most general reactions, (1)–(13), for the process according to Miller.³

Because the absorber promotes reaction as well as mass transfer, ASPEN PLUS's reactive-distillation model describes it mathematically.

In addition to reactions (1)–(13) listed in Table 1, we also need to consider the action of electrolytes in the

absorber. The high absorption capacity of NO_x stems from the high thermodynamic stability of aqueous nitric acid, the final product of NO_x absorption. This stability, in turn, results from the dissociation of the acid to the nonvolatile nitrate ion, NO₃⁻. As a strong acid, aqueous nitric acid exists mostly as NO₃⁻.

ASPEN PLUS's electrolyte, nonrandom-two-liquid (NRTL) thermodynamic model includes electrolyte actions in the absorber's aqueous environment. This model requires all electrolytic reactions to be specified; for our problem, the key reaction is



Although the reaction is labeled "global" in the simulation (occurring in all units), it must also appear as a reactive-distillation reaction in the absorber stages. Otherwise, ASPEN PLUS assumes that the reaction does not occur in the absorber.

Applying the assumptions described in the following sections to the reactions listed in Table 1 produces a practical model for the NO_x absorption at RFAAP. These

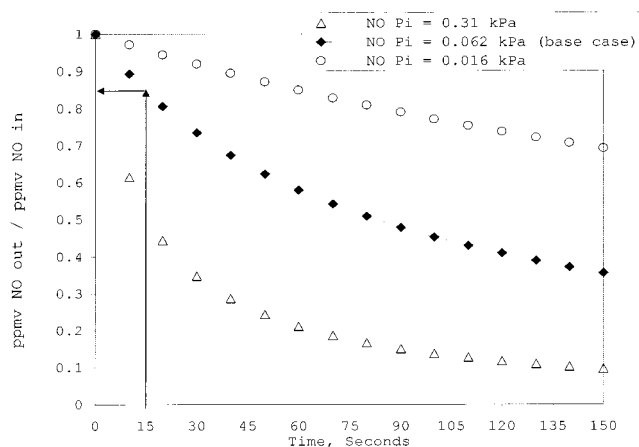


Figure 2. Transient oxidation of NO via reaction (1) for various initial partial pressures.

assumptions stem from the relative importance of certain reactions and components, and the simulation's realistic performance (sections 7 and 8) validates them.

4.1. Assumption I: Inclusion of Reaction (1) as a Kinetic Rate Equation. Reaction (1), the oxidation of NO to NO₂, remains important in NO_x chemistry. In cases where NO represents the major contributor to the total NO_x, it has been identified as a major rate limitation in the overall absorption mechanism according to Miller.³ In other words, reaction (1) is critical when producing NO₂ from NO oxidation. Such is the case in nitric acid production, where ammonia oxidizes to NO under high pressure, which in turn oxidizes to NO₂. However, at RFAAP, NO_x fed to the system consists mostly of NO₂, making the reaction less critical.

Because the oxidation of NO is irreversible according to Miller,³ we treat reaction (1) as a forward reaction only. Using reaction-rate data presented by Suchak and Joshi,⁴ we calculate the time-dependent change of the fraction of entering NO oxidized by reaction (1) (preexponential = 1.814×10^{-3} kPa⁻¹ and activation energy = 1.658 kcal/g·mol). Figure 2 shows the results at varying NO partial pressures for the starting conditions of the fume feed to the bottom of the column. With a gas flow rate of 113.3 CMM (4000 standard cubic feet per minute, SCFM) through the column, the total void volume allows a residence time of 15 s. According to Figure 2, less than 15% of the NO oxidizes to NO₂. This result, together with the fact that NO₂ represents the major component of the total NO_x fed to the absorber, justifies elimination of reaction (1) in similar cases. However, for completeness, we include reaction (1) in the model.

4.2. Assumption II: Treatment of Reaction (2) as Being in an Instantaneous Equilibrium. Reaction (2), $2\text{NO}_2 = \text{N}_2\text{O}_4$, proceeds quickly and reversibly and equilibrates rapidly according to Miller³ and Matasa and Tonca.⁵ Because it typically achieves equilibrium in 0.0001 s,⁵ it is effectively in equilibrium instantaneously with respect to other time-dependent concentrations. Therefore, although the two compounds cannot be isolated, we can always determine the concentration of NO₂ and N₂O₄ from the total NO₂ + N₂O₄. In this work, NO₂* denotes NO₂ + 2N₂O₄.

4.3. Assumption III: Combination of Reactions (4) and (5). Reactions (4) and (5) are fast and equilibrate rapidly in the liquid film, especially for tray absorbers as is the case at RFAAP. Miller³ and others suggest representing them in combination, yielding the

following reaction, (4–5), at equilibrium in the liquid phase:



4.4. Assumption IV: Elimination of HNO₂. Several factors support elimination of HNO₂. First, combining reactions (4) and (5) (assumption III) to eliminate the intermediate HNO₂ according to Miller³ implies that the concentration of HNO₂ remains very low and relatively constant because reaction (5) consumes it as soon as reaction (4) produces it. HNO₂ does not exist for extended periods because it is a very unstable compound. Second, literature data for the liquid-phase oxidation of HNO₂ [reaction (9): $2\text{HNO}_2 + \text{O}_2 = 2\text{HNO}_3$] remain unavailable,³ and the liquid-phase concentration of O₂ is very low. Therefore, we can neglect the effect of HNO₂ oxidation in the liquid-phase reactions, (8) and (9).

4.5. Assumption V: Treatment of Reaction (6) as Being in an Instantaneous Equilibrium. The association of NO and NO₂ molecules to produce N₂O₃ [reaction (6)] is much slower than reaction (2), equilibrating in 0.1 s [versus 0.0001 s for reaction (2)].⁵ In addition, N₂O₃ is much less stable than N₂O₄ according to Miller.³ The assumption of equilibrium levels of N₂O₄ and N₂O₃ gives an appreciable amount of N₂O₄ but very little N₂O₃. At the absorber inlet, there is approximately 100 times more N₂O₄ than N₂O₃ (4.8×10^{-2} kg·mol/h N₂O₄ versus 4.1×10^{-4} kg·mol/h N₂O₃).

Some researchers (e.g., Thomas and Vanderschuren⁶) claim that the N₂O₃ pathway dominates, but this applies only in systems with higher pressures and higher NO-to-NO₂ ratios. In these cases, N₂O₃ can outstrip N₂O₄ and also certainly absorbs faster than NO or NO₂. Given that N₂O₄ exists in higher concentrations and thus will absorb and react at a faster rate, N₂O₃ absorption represents a secondary mechanism in NO_x absorption. In the case of RFAAP, we can neglect the N₂O₃ pathway with minimal effect on the simulation accuracy. However, we will include the production and absorption of N₂O₃ for the sake of completeness.

If we combine reactions (8) and (5) to eliminate transient HNO₂ as we did with reaction (4–5) and multiply the reaction by 2, the result becomes



We rewrite this reaction as



where 3NO cancels on each side of the equation, leaving us with reaction (4–5) with 6NO₂ replaced with 3N₂O₄.

4.6. Assumption VI: Neglect of the Vapor-Phase Acid Production. Because researchers typically treat the vapor-phase production of nitric and nitrous acids as negligible,³ we can neglect reaction (10). Note that the mass-transfer reaction (12) for HNO₃ will remain.

4.7. Assumption VII: Treatment of Reaction (13). NO₂ has a lower solubility and reactivity than N₂O₄. Suchak and Joshi⁴ state that absorption of NO₂ as such is negligible. Similarly, Miller³ says that the NO₂ routes are slow relative to those involving the reactants N₂O₄ and N₂O₃ and can usually be neglected in evaluating the nitric acid absorption performance. Newman and Carta⁷ state that "the absorption of NO₂ in water has been studied extensively. All studies indicate that at

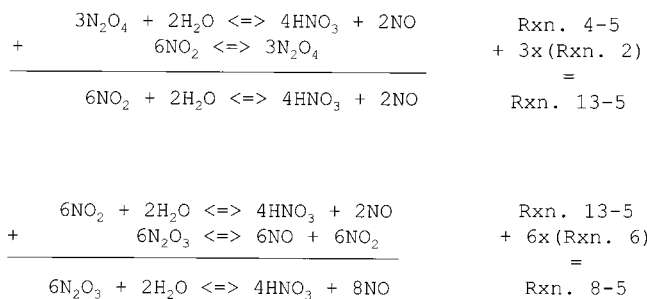


Figure 3. Illustration of the equilibrium conditions for the three NO_x pathways.

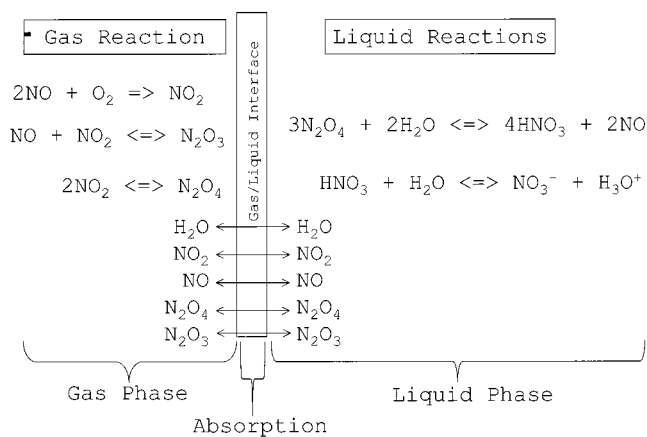


Figure 4. Final reaction and absorption mechanism after the application of assumptions I–VII.

partial pressures of NO_2 greater than about 0.2 kPa (0.002 atm) the absorption...occurs via N_2O_4 ." The partial pressure of NO_2 in the fume feed at RFAAP is 0.5 kPa (0.005 atm). If we combine reactions (13) and (5) to eliminate transient HNO_2 and multiply the reaction by 2, we obtain reaction (13–5). We see that



this reaction is simply reaction (4–5) after replacing 6NO_2 with $3\text{N}_2\text{O}_4$.

4.8. Final Reaction Set. Figure 3 illustrates the concepts described in assumptions V and VII. The equilibrium conditions of the reactions in the different pathways allow manipulation of the equations as shown in the figure. In this way, we have accounted for the complex equilibria of the three distinct pathways by applying the above assumptions.

After assumptions I–VII are applied, the overall reaction mechanism simplifies to the one shown in Figure 4. We note that the validity of the simplified reaction set proposed here depends on a high liquid residence time at each column stage, as is the case in tray absorbers. The resulting approximation of the liquid-phase reaction equilibrium allows the application of assumptions III, V, and VII. In the cases of packed and spray absorption towers, the inaccuracy of the equilibrium approximation requires the treatment of hydrolysis reactions (4), (8), and (13) with the decomposition reaction (5) as kinetic reactions.

ASPEN PLUS calculates vapor–liquid equilibrium in the absorber, so all species are capable of interfacial mass transport. However, by far the most important mass-transfer component is N_2O_4 , which must absorb into the aqueous phase before reacting. Also note that excess NO can, by mass action, absorb and push reaction

Table 2. Parameter Values for the Reduction of NO and NO_2 with Ammonia

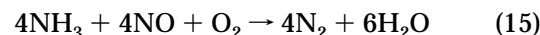
symbol	units	value	source
A_1	$\text{kg}\cdot\text{mol}/(\text{s}\cdot\text{m}^3)$	15×10^6	<i>a</i>
E_1	$\text{kcal}/\text{g}\cdot\text{mol}$	15	<i>b</i>
<i>a</i>	unitless	1	<i>b</i>
<i>b</i>	unitless	0.5	<i>b</i>
<i>c</i>	unitless	5×10^{-4}	<i>d</i>
p_{NO}	kPa	<i>c</i>	
p_{O_2}	kPa	<i>c</i>	
p_{NH_3}	kPa	<i>c</i>	
A_2	$\text{kg}\cdot\text{mol}/(\text{s}\cdot\text{m}^3)$	15×10^6	<i>e</i>
E_2	$\text{kcal}/\text{g}\cdot\text{mol}$	14.5	<i>e</i>
<i>x</i>	unitless	1	<i>e</i>
<i>y</i>	unitless	0.5	<i>e</i>
<i>z</i>	unitless	5×10^{-4}	<i>e</i>
p_{NO_2}	kPa	<i>c</i>	
A_3	$\text{kg}\cdot\text{mol}/(\text{s}\cdot\text{m}^3)$	15×10^6	<i>e</i>
E_3	$\text{kcal}/\text{g}\cdot\text{mol}$	10	<i>e</i>
<i>m</i>	unitless	1	<i>e</i>
<i>n</i>	unitless	5×10^{-4}	<i>e</i>
A_4	$\text{kg}\cdot\text{mol}/(\text{s}\cdot\text{m}^3)$	0.1	<i>e</i>
E_4	$\text{kcal}/\text{g}\cdot\text{mol}$	10	<i>e</i>
<i>d</i>	unitless	0	<i>e</i>
<i>e</i>	unitless	0.3	<i>e</i>
$p_{\text{H}_2\text{O}}$	kPa	<i>c</i>	
p_{N_2}	kPa	<i>c</i>	

^a Willi et al.⁹ ^b Marangozis.¹⁰ ^c Denotes that the value varies depending on feed and catalyst-vessel operating conditions. ^d Most research suggests zero order with respect to NH_3 ; however, the minimal value shown here ensures the cessation of reaction upon exhaustion of the NH_3 supply. ^e These values for equations (19)–(21) were assumed based on the data for eq 18.

(4–5) back to their reactants. Because reaction (4–5) is in equilibrium and NO_2 and N_2O_3 are active in the system, we also consider these NO_x components in the reaction mechanism shown in Figure 4.

5. Selective Catalytic Reduction

We now turn to the catalyst vessel unit. In the presence of a saturating level of oxygen, reactions (15)–(17) represent the mechanism in the SCR.



Equations (18)–(20) describe the forward rates of reactions (15)–(17), respectively, and Table 2 summarizes the corresponding parameter values. The re-

$$-4\text{d}[\text{NO}]/\text{d}t = A_1 e^{-E_1/RT} p_{\text{NO}}^a p_{\text{O}_2}^b p_{\text{NH}_3}^c \quad (18)$$

$$-2\text{d}[\text{NO}_2]/\text{d}t = A_2 e^{-E_2/RT} p_{\text{NO}_2}^x p_{\text{O}_2}^y p_{\text{NH}_3}^z \quad (19)$$

$$-4\text{d}[\text{NO}]/\text{d}t = A_3 e^{-E_3/RT} p_{\text{NO}}^m p_{\text{NH}_3}^n \quad (20)$$

verse of reaction (15) accounts for the effect of water on the SCR reactions, as described by Willi et al.⁹ Kinetic equation (21) mathematically describes this reaction.

$$4\text{d}[\text{NO}]/\text{d}t = A_4 e^{-E_4/RT} p_{\text{H}_2\text{O}}^d p_{\text{N}_2}^e \quad (21)$$

6. Absorption Simulation Results

6.1. Comparison to Design Specifications. Tables 3 and 4 compare the model results for key flow streams

Table 3. Gas- and Liquid-Outlet Streams from the Absorber

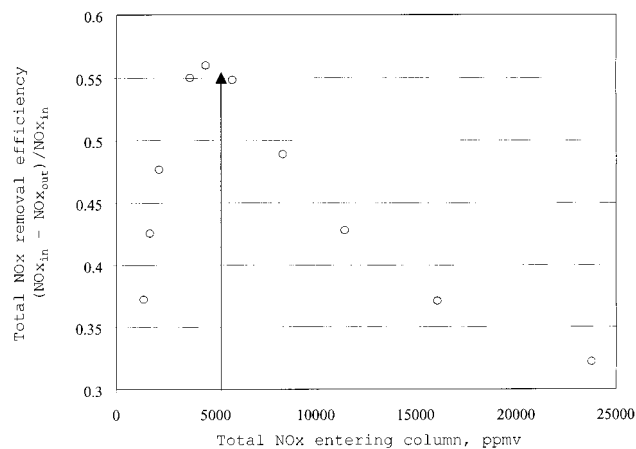
data source	RFAAP data	model	RFAAP data	model
stream	fume from top	fume from top	acid from bottom	acid from bottom
component mole flow (concentration)	kg-mol/h (ppmv)	kg-mol/h (ppmv)	kg-mol/h	kg-mol/h
NO	0.63 (2127)	0.65 (2195)		
NO ₂	0.12 (405)	0.12 (401)		
total NO _x	0.75 (2532)	0.76 (2598)		
HNO ₃	trace	0.00	0.95	0.937
O ₂	59.9	60.0		
N ₂	225.6	225.6		
H ₂ O	9.9	9.2	5.9	6.4
total flow, kg-mol/h	296.2	295.5	9.4	8.24
total flow, kg/h	8440.4	8430.5	170.5	190.9
temperature, °C	26.7	26.0	30.0	31.4
pressure, kPa	96.5 ^a	96.5 ^a	413.7 ^b	413.7 ^b
acid wt %			35.2	30.9

^a Column run at ambient pressure. High-altitude operation dictates a pressure lower than 101.325 kPa. ^b Bottoms pressure measured at acid pump discharge.

Table 4. Stream Results for the Kinetic Model As Compared to RFAAP Data

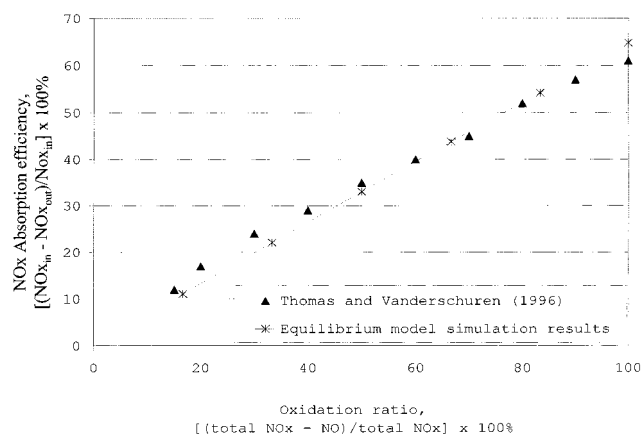
data source	RFAAP data	kinetic model
stream	gas to vent stack (SCR output)	gas to vent stack (SCR output)
component mole flow (concentration)	kg-mol/h (ppmv)	kg-mol/h (ppmv)
NO	0.027 (91)	0.028 (96)
NO ₂	trace	0.002 (4)
total NO _x	0.027 (91)	0.031 (100)
NH ₃	trace	0.037
O ₂	59.9	59.9
N ₂	225.3	226.3
H ₂ O	10.8	10.4
total flow, kg-mol/h	297.0	296.6
total flow, kg/h	8450.9	8445.0
temperature, °C	177	177
pressure, kPa	97	103

Note: The kinetic model uses the same input NH₃ as RFAAP at 0.621 kg-mol/hr.

**Figure 5.** Plot of NO_x removal efficiency vs total NO_x fed to the column. The arrow locates the inlet NO_x concentration (5200 ppmv) to the absorber at RFAAP.

to the RFAAP design specifications. As the tables show, the simulation agrees quite closely with design specifications.

6.2. Comparison to Literature Data. Direct comparisons for simulation results for NO_x absorption with literature data remain elusive because of the number of variables affecting the system and the difficulty of locating literature data with similar experimental conditions. For example, the removal efficiency versus inlet NO_x concentration (ppmv), shown in Figure 5, exhibits a clear maximum in the data. In fact, the operating

**Figure 6.** Comparison of absorption results to those of Thomas and Vanderschuren.⁸

range of the absorber at RFAAP passes directly through this maximum. The shift in this maximum with respect to different process variables produces either a positive or negative effect of the inlet NO_x concentration on removal efficiency.

Physically, this maximum marks the transition between absorption limited by the gas concentration to that by the liquid concentration. At low NO_x concentrations, the concentrations of vapor-phase reaction products are low. Thus, the rate of absorption of these species proceeds slowly. As NO_x concentrations increase, more NO₂ exists as the more readily absorbed N₂O₄. Eventually, the equilibrium nitric acid concentration in the scrubbing liquid begins to limit absorption as the backward reactions and desorption of species from the liquid increase. The location of this maximum can, in fact, move along the *x* axis. Many variables, including the water flow rate, temperature, and pressure, affect the location of this transition point.

A second key area for comparison is the oxidation ratio, which is essentially the ratio of NO₂ and N₂O₄ to the total NO_x. Figure 6 compares the model's performance to results presented by Thomas and Vanderschuren.⁸ We compared a single equilibrium stage in our model to the results of a small bench-scale packed column used by Thomas and Vanderschuren. We use temperatures, pressures, and inlet NO_x concentrations identical with those of the experimental column for our simulation. The gas residence times for the simulation and the experimental column were comparable with 3.0 and 2.6 s, respectively. The model's sensitivity to the NO_x oxidation ratio agrees with the literature. We see

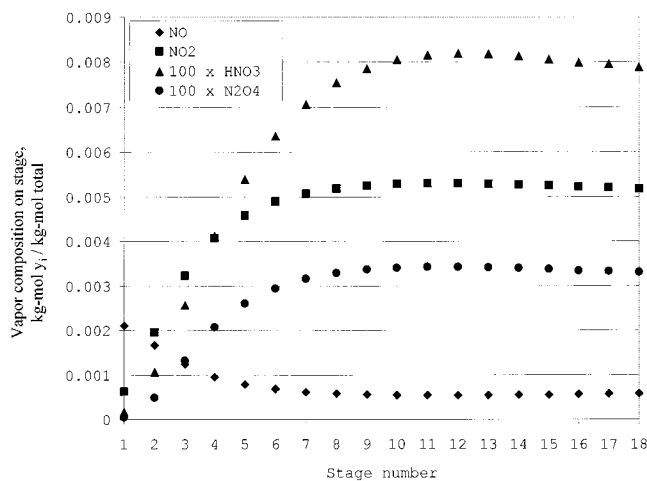


Figure 7. Simulation results for vapor-component stage compositions for the absorber for the equilibrium model. Top = 1. Bottom = 18.

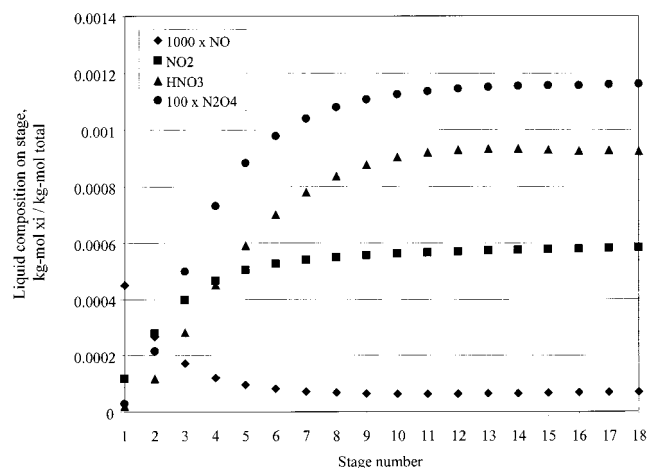


Figure 8. Simulation results for liquid-component stage compositions for the absorber for the equilibrium model. Top = 1. Bottom = 18.

that, at the 100% oxidation ratio, the NO_x absorption efficiency approaches the “ $2/3$ ” limit described by Cheremisinoff and Young.¹ This limit derives from the stoichiometry of reaction (4–5). If the reaction proceeds to completion, then, for every 3 kg·mol of NO_2 ($1/2\text{N}_2\text{O}_4$) absorbed, 1 kg·mol of NO is produced, thereby effectively yielding only 2 kg·mol of overall NO_x absorption. In actuality, equilibrium ensures that this limit is approached but never reached.

6.3. Practical Implications. Figures 7 and 8 show the vapor- and liquid-composition profiles, respectively, for each of the 18 stages. Most of the NO_x absorption (identified by the change in concentration) occurs at the top of the column, where the pure filtered water feed creates the greatest driving force. Water flowing down through the column becomes increasingly fortified in nitric acid until it reaches a limiting concentration that precludes further absorption. Hence, little additional absorption occurs below stage 10.

In practice, spikes in the NO_x content of the absorber feed inevitably occur. The simplest remedy is to increase the freshwater feed to the tower, diluting the nitric acid in the bottom and increasing the driving force for NO_x absorption. Theoretically, a new feedback controller could add water based on the NO_2 outlet from the tower, as shown in Figure 9.

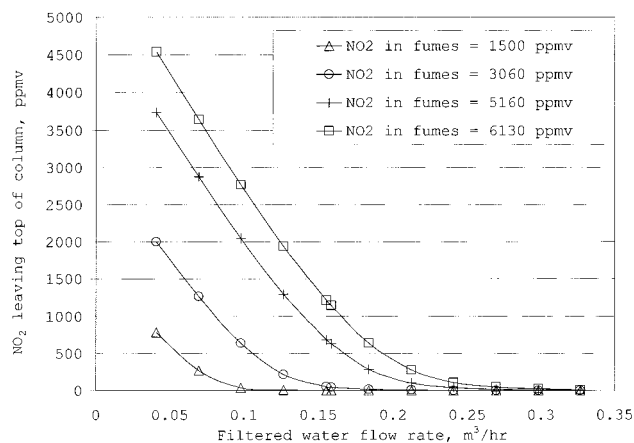


Figure 9. Plot of NO_2 out the top of the column vs filtered water fed to the column for varying NO_2 concentration in fume ($1 \text{ m}^3/\text{h}$, 4.4 gpm).

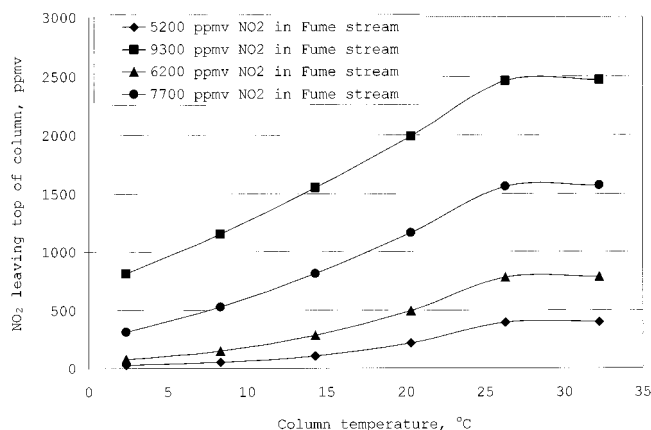


Figure 10. Plot of NO_2 out of the top of the column vs fume feed temperature to column (simulating a cooling jacket).

A second option involves temperature control: reducing the absorber temperature improves NO_x absorption dramatically. If the operator can control the temperature of the fume feed, a feedback control loop can monitor the NO_x content exiting in the gas stream and cool the fume feed to the temperature required to achieve the desired NO_x outlet concentration, as shown in Figure 10. This figure shows NO_2 inlet rates to the column of 1.5, 1.8, 2.3, and 2.7 kg·mol/h.

In the case of RFAAP, the fume feed rate greatly exceeds the water feed rate to the column. Therefore, the water feed to the column has a negligible effect on the column temperature relative to the fume feed. Adding a heat exchanger to the fume feed stream is a less expensive retrofit than adding a cooling jacket or cooling trays to an existing column. New designs should explore the use of these alternatives for column cooling, especially if the water flow rate is low relative to the gas flow rate.

7. SCR Simulation Results

7.1. Optimum Ammonia-to- NO_x Feed Ratio. The fume outlet of the absorber, after heating and mixing with ammonia, becomes the feed to the SCR catalyst vessel. Key factors in SCR performance include the NO_x concentration, ammonia-to- NO_x feed ratio, and oxygen feed concentration. Because the catalyst vessel temperature is tightly controlled between 305 and 325 °C (both for safety and for avoidance of undesirable reactions),

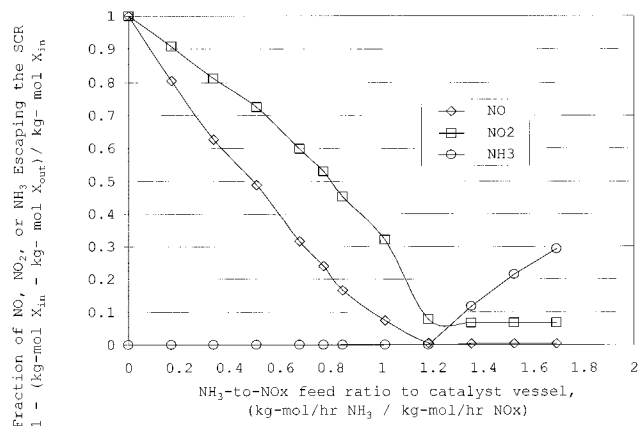


Figure 11. Plot of the fraction of the feed that escapes the catalyst vessel versus the ammonia-to-NO_x feed ratio.

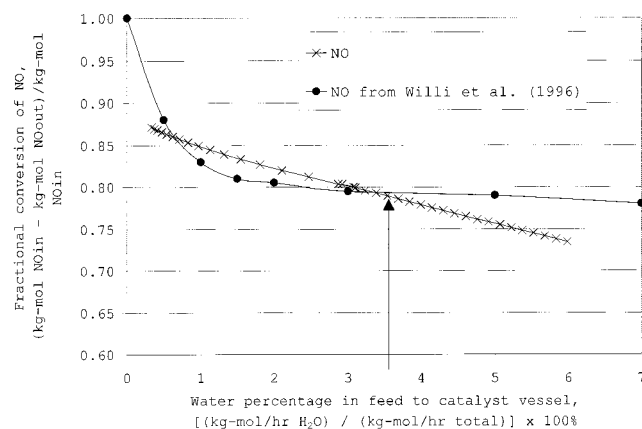


Figure 12. Plot of the effect of water in the feed on the fractional conversion of NO compared to the results of Willi et al.⁹

it has little effect on performance over this narrow range.

Figure 11 shows the effect of the ammonia feed ratio on the NO_x reduction efficiency for the SCR model. Optimal NO_x removal occurs at an NH₃-to-NO_x feed ratio of 1.2. Typically, the optimum ratio is 1.0; however, because 1 mol of NO₂ requires 2 mol of NH₃ to react, appreciable amounts of NO₂ in the system boost the NH₃ requirement so that mixtures of NO and NO₂ require a ratio greater than 1.0. The optimum ratio can only be determined by studying each system; in all cases, though, strict feedback control should be used to minimize both NO_x and ammonia slip.

7.2. Comparison to Literature Data. Figure 12 compares the model's response to water in the SCR feed to results published by Willi et al.⁹ Although the model shows a systematic deviation, it does predict the general trend and provides an effective approximation in the relevant operating range. Importantly, water in the SCR feed stream appears to be an issue at RFAAP; the arrow in Figure 12 marks the current water content (3.6% by mole).

This problem, stemming from the upstream water absorber, highlights the importance of viewing the entire abatement system holistically. Cooling the absorber column would condense more water and, consequently, pass less to the SCR. RFAAP should consider this option, especially if Willi et al.⁹ are correct in that some of the effects of water represent irreversible damage to the catalyst. Equally important, while Figure 12 presents results for a fully functional catalyst, years

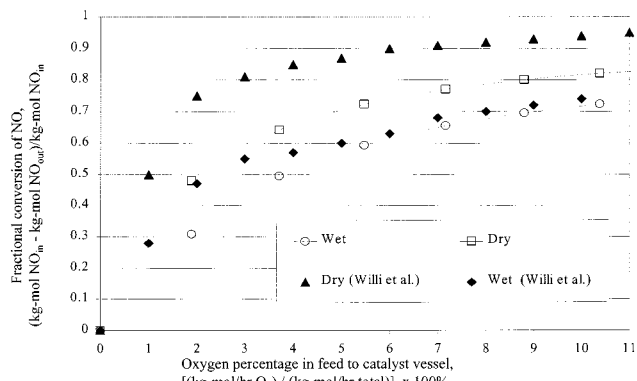


Figure 13. Plot of the effect of oxygen in the feed on the fractional conversion of NO for the simulation presented in comparison to data of Willi et al.⁹

of use as well as contamination from acids and liquid water degrade the catalyst performance considerably. Consequently, the catalyst activity level must be tested periodically to predict the performance and schedule refurbishment.

Figure 13 shows the effect of oxygen on the feed for dry and wet gas streams in both the model and Willi et al.⁹ Again, the model's trend matches the reported results, with the error considered a small shift downward in performance. The discrepancy is largest at low oxygen concentrations, where its effect is greatest. The error stems from differences between the model and the literature in terms of both NO_x feed concentration and catalyst vessel size, though again in both cases the results are for a pristine catalyst.

The SCR at RFAAP runs at 20% oxygen in the gas feed, safely above the point of diminishing returns, though hardly by design. As noted previously, large quantities of entrained air hinder the absorber performance upstream. For situations with limiting oxygen levels, any air fed to the catalyst vessel should be minimized.

8. Retrofit Options

Aside from very expensive catalyst refurbishment, the SCR at RFAAP is running at near optimum conditions, and the strict safety limits on temperatures and the ammonia feed ratio preclude most retrofit design options. Therefore, the following options directly address only the absorber, with downstream effects noted where applicable.

8.1. Column Cooling. Cooling the column improves nearly all aspects of NO_x absorption. Remarkably, all important equilibrium reactions are exothermic. Reaction (1), the only rate-limiting reaction, actually proceeds faster as the temperature decreases (quite unique in the study of kinetics). Therefore, cooling the process has few disadvantages. The primary problem is finding a feasible way to apply the theory. The most promising method appears to be cooling the fume stream with chilled water or using an acid-resistant chiller to cool the high-flow-rate scrubber liquid recycle. Figure 14 shows the simulation results for the first option. With a cooled gas stream, the downstream heaters must provide additional heat to maintain the optimal SCR reaction temperature. This heat can easily come from increasing either the steam to the steam preheater or the natural gas to the direct-fired heater.

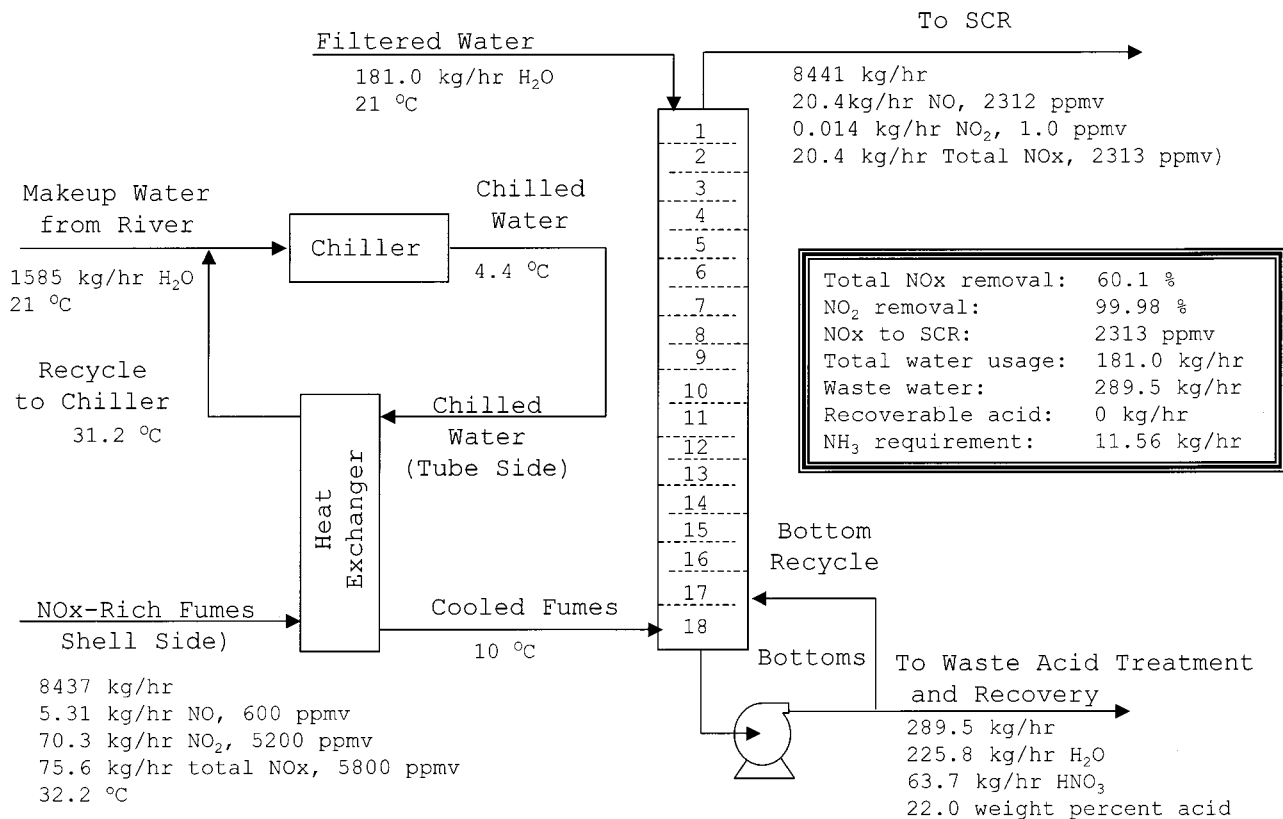


Figure 14. Block flow diagram of the NO_x abatement system utilizing fumes cooling.

Column cooling also dilutes the recoverable acid by condensing water that otherwise would leave the column in the gas stream, creating a second economic drawback. This problem is important for nitric acid plants where acid is easily recovered but less so for applications that do not have the infrastructure for recovery.

Finally, column cooling also significantly benefits the downstream SCR. With more water condensing and leaving in the liquid bottoms, less water enters the catalyst vessel, which improves the SCR reaction (Figure 12) and reduces catalyst damage.⁹

8.2. Acid Flash. Although the relatively low temperatures in the SCR (as well as the relative isolation of the SCR at RFAAP) preclude heat integration, the stack gas offers a ready source of energy for the NO_x abatement system. One novel way to handle the effects of additional water on acid recovery, for example, is with a flash drum to concentrate the acid. Figure 15 shows the simulation results for this scenario. At RFAAP, the minimum acid concentration offering feasible recovery is 30 wt %; as the results show, a single-stage flash drum can achieve this concentration with no other modifications beyond a lower filtered water requirement.

The costs are piping, equipment, and transportation of the recovered acid to the nitric acid plant on site. The added benefit is that controlling the filtered water flow rate becomes less critical, making it easy to add water to cover fluctuations in NO_x input. In addition, if desired, the gas flow from the top of the absorber can cool the water vapor leaving the flash drum as well as slightly preheat the gas stream destined for the SCR. A multiple-stage flash would minimize the filtered water requirement.

9. Retrofit Economics

Table 5 presents the economics for the key retrofit options relative to the base case/current situation at RFAAP. When economics are evaluated, however, it is important to remember that traditional payback times may have little relevance in pollution-control discussions. Rules and regulations of the EPA and VDEQ, along with the fines for noncompliance, change constantly. Consequently, it may be misleading to calculate payback times solely from assumptions for the required engineering design and skilled labor work plus estimates for the cost of piping, equipment, and materials. Cooling the fume feed is a case in point; this retrofit has no payback time because the annual costs are higher than those of the base case. Yet, such a retrofit may prove invaluable in meeting EPA and VDEQ requirements.

In other words, the absence of a direct payback period for the retrofit does not take into account the insurance it provides against fines levied for excess NO_x emissions. Should the base-case performance prove subpar, it does not take many \$25 000/day fines to make the retrofit more economically feasible. One thing we know for certain is that governmental agencies are not relaxing their emission limits on NO_x and other pollutants; these limits will only become tighter in the future, and companies need to be prepared to handle the restrictions if they want to avoid costly fines and penalties.

10. Observations for NO_x Abatement Utilizing Absorption and SCR

Using equilibrium reactions to model NO_x absorption and using kinetic reactions to model the SCR agree sufficiently with both design specifications and literature data for the conditions encountered at RFAAP.

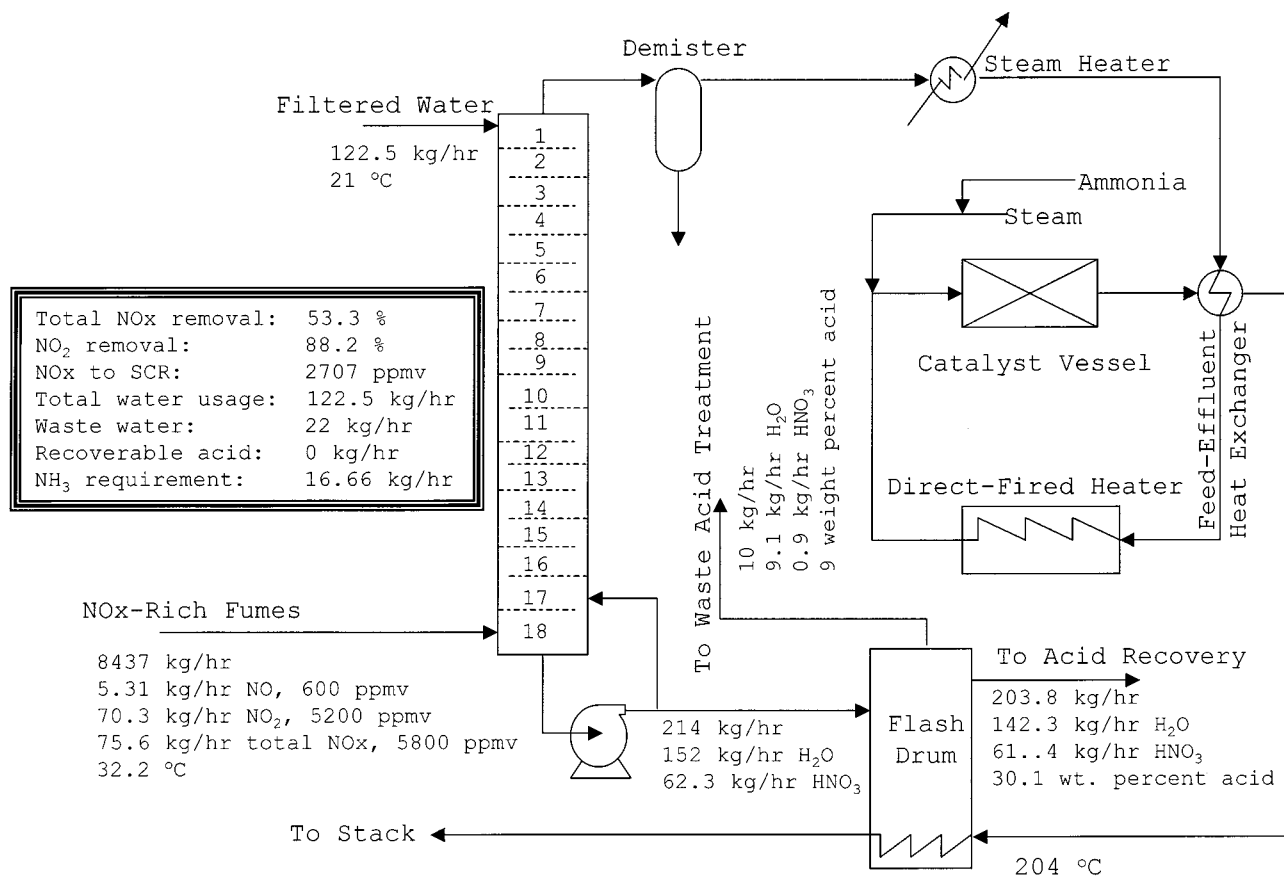


Figure 15. Block flow diagram of the NO_x abatement system implementing acid flash.

Table 5. Process Retrofit Economics^{11,12}

capital investments/costs/recoveries	base case		I: cooling the fume stream		II: acid flash	
	amount	cost, \$	amount	cost, \$	amount	cost, \$
Equipment/Fixed Costs						
pump				1095		1095
tank						
heat exchanger				16428		3286
chiller				13142		
column mod.						
H ₂ O ₂ storage/plant						
piping, installed (m)			100	4922	100	4922
engineering (h)			80	4000	80	4000
skilled labor (h)			80	2000	80	2000
total fixed costs				41587		15302
Annual Operating Costs						
process water (cm ³)	1.40 × 10 ³	404	8.00 × 10 ²	231	2.30 × 10 ³	658
slaked lime (kg)	5.30 × 10 ⁵	24861	5.30 × 10 ⁵	24917	5.30 × 10 ⁴	2492
cooling water (cm ³)			3.70 × 10 ⁶	135983	2.30 × 10 ⁵	8567
refrigeration (mJ)			9.20 × 10 ¹⁰	666		
electricity (kW-h)			1.80 × 10 ⁵	8635		
steam (kg)					4.70 × 10 ⁵	2681
total annual operating costs		25265		170432		14398
recovered acid (kg)					4.70 × 10 ⁵	2499
annual costs minus recoveries		25265		170432		11899
payback time (years)						1.14

(i) Controlling the temperature, pressure, and filtered-water feed rate can greatly improve NO_x absorption in the scrubber absorber.

(ii) These dramatic improvements in NO_x absorption (pressure, cooling, and increased water input) dilute the bottom acid product.

(iii) Each temperature and pressure state within the column has a limiting NO_x absorption based on a nitric acid concentration above which no NO_x absorbs.

(iv) Because slow mass-transfer rates represent a major limiting step in NO_x absorption, it is important

to investigate ways to improve mass transfer, such as replacing bubble-cap trays with sieve trays.

(v) Diluting NO_x in an inert gas slows its absorption in the absorber and its reduction in the SCR because of concentration-dependent reactions in both units. Consequently, although oxygen improves the SCR reaction downstream, entrained air in NO_x gas destined for absorption should be minimized.

(vi) Oxygen is important to successful SCR operation, and although its contribution to NO_x absorption is

minimal in this case, it becomes more important at higher NO partial pressures.

(vii) Water has a marked deleterious effect on SCR operation, both transient and permanent. Preceding the SCR with absorption increases the risk of water damage to the SCR catalyst. Designers should take steps to minimize water intrusion to the catalyst vessel.

Beyond developing specific conclusions, however, the practical reaction mechanism presented, built using readily available process simulation software, should offer a sense of empowerment. Ideally, the method for developing the mechanisms for NO_x absorption and SCR transcends these two processes alone; the logic and information here can serve as a starting point for developing usable models for other situations, again, always taking the particulars of each scenario into account.

Acknowledgment

We gratefully acknowledge the support of this work by the Alliant Techsystems, contract operator of the Radford Facility and Army Ammunition Plant, Radford, VA. We also thank the Honeywell International Foundation and Aspen Technology, Inc. (in particular, Dr. Jita Mahalec, Director, Worldwide University Programs), for supporting the computer-aided design educational program at Virginia Tech.

Nomenclature

a = reaction order with respect to NO, eq 18
 A_1 = preexponential factor, eq 18, kg·mol/(s·m³)
 A_2 = preexponential factor, eq 19, kg·mol/(s·m³)
 A_3 = preexponential factor, eq 20, kg·mol/(s·m³)
 A_4 = preexponential factor, eq 21, kg·mol/(s·m³)
 b = reaction order with respect to O₂, eq 18
 c = reaction order with respect to NH₃, eq 18
 CMM = cubic meters per minute, m³/min
 d = reaction order with respect to H₂O, eq 21
 e = reaction order with respect to N₂, eq 21
 E_1 = activation energy, eq 18, kcal/g·mol
 E_2 = activation energy, eq 19, kcal/g·mol
 E_3 = activation energy, eq 20, kcal/g·mol
 E_4 = activation energy, eq 21, kcal/g·mol
 E_v = vaporization efficiency
 m = reaction order with respect to NO, eq 20
 n = reaction order with respect to N₂, eq 20
 NO₂* = total NO₂ species (NO₂ + N₂O₄)
 $p_{\text{H}_2\text{O}}$ = H₂O partial pressure, kPa

p_{N_2} = N₂ partial pressure, kPa

p_{NH_3} = NH₃ partial pressure, kPa

p_{NO} = NO partial pressure, kPa

p_{NO_2} = NO₂ partial pressure, kPa

p_{O_2} = O₂ partial pressure, kPa

ppmv = parts per million by volume

scfm = standard cubic feet per minute, ft³/min

wt % = HNO₃ absorber liquid outlet weight percent, kg of HNO₃/kg of the total

x = reaction order with respect to NO₂, eq 19

y = reaction order with respect to O₂, eq 19

z = reaction order with respect to O₂, eq 19

Literature Cited

- (1) Cheremisinoff, P. N.; Young, R. A., Eds. *Air Pollution Control and Design Handbook*; Marcel Dekker: New York, 1977; Part 2, pp 628 and 671–678.
- (2) Cho, S. M. Properly Apply Selective Catalytic Reduction for NO_x Removal. *Chem. Eng. Prog.* **1994**, 90 (No. 1), 39.
- (3) Miller, D. N. Mass Transfer in Nitric Acid. *AIChE J.* **1987**, 33, 1351.
- (4) Suchak, N. J.; Joshi, J. B. Simulation and Optimization of NO_x Absorption System in Nitric Acid Manufacture. *AIChE J.* **1994**, 40, 944.
- (5) Matasa, C.; Tonca, E. *Basic Nitrogen Compounds: Chemistry, Technology and Applications*, 3rd ed.; Chemical Publishing Co., Inc.: New York, 1973; p 44.
- (6) Thomas, D.; Vanderschuren, J. Modeling of NO_x Absorption into Nitric Acid Solutions Containing Hydrogen Peroxide. *Ind. Eng. Chem. Res.* **1997**, 36, 3315.
- (7) Newman, B. L.; Carta, G. Mass Transfer in the Absorption of Nitrogen Oxides in Alkaline Solutions. *AIChE J.* **1988**, 34, 1190.
- (8) Thomas, D.; Vanderschuren, J. The Absorption–Oxidation of NO_x with Hydrogen Peroxide for the Treatment of Tail Gases. *Chem. Eng. Sci.* **1996**, 51, 2649.
- (9) Willi, R.; Roduit, B.; Koepfel, R. A.; Wokaun, A.; Baiker, A. Selective Reduction of NO by NH₃ over Vanadia-Based Commercial Catalyst: Parametric Sensitivity and Kinetic Modeling. *Chem. Eng. Sci.* **1996**, 51, 2897.
- (10) Marangozis, J. Comparison and Analysis of Intrinsic Kinetics and Effectiveness Factors for the Catalytic Reduction of NO with Ammonia in the Presence of Oxygen. *Ind. Eng. Chem. Res.* **1992**, 31, 987.
- (11) Peters, M. S.; Timmerhaus, K. D. *Plant Design and Economics for Chemical Engineers*, 4th ed.; McGraw-Hill: New York, 1991; pp 661–677.
- (12) Marshall and Swift Equipment Cost Index. *Chem. Eng.* **1999**, May.

Received for review June 1, 2000

Revised manuscript received March 21, 2001

Accepted March 26, 2001

IE0005295